Fabrication and Thermoelectric Properties of Ultrathin Layer of $Mo_{1-x}Nb_xS_2$

Koyano Laboratory

1440012

PHAM, Thi Xuan

Background of research

Thermoelectric (TE) technology which converts waste heat directly into electrical energy using power generators, and vice versa using Peltier coolers has attracted much attention for decades. The conversion efficiency of the TE materials can be evaluated by power factor $PF = S^2\rho^{-1}$ and the dimensionless figure of merit $ZT = (S^2T)/(\rho\kappa)$, where S is the Seebeck coefficient, ρ is electrical resistivity, κ denotes thermal conductivity, and T is temperature [1]. However, the intrinsically compromised behavior between S, ρ and κ causes a challenging issue for the enhancement of efficiency [2].

In the 1990s, Hicks and Dresselhaus [3] proposed the potential of low-dimensional TE materials with high ZT because of the enhancement of S caused by quantum confinement and the decrease of κ caused by the increase of surface scattering. Their idea combined with recent remarkable advances in two-dimensional (2D) materials, has spurred studies examining TE applications [4]. Among them, 2D MoS_2 is the candidate for TE investigation because it has not only high power factor but also unique properties for TE devices [5], such as high mechanical flexibility and in-plane mechanical stiffness. However, the large PF of n-type MoS_2 ultrathin layers obtained in the field effect transistor (FET) structure produces a complicated technique for device fabrication and creates difficulty for TE applications. Moreover, the TE properties of the p-type doped MoS_2 ultrathin layers, which are fundamentally necessary for TE devices that consist of n-type and p-type TE elements [6], have not been studied.

Purpose

In this research, I investigate the TE properties of Nb-doped MoS_2 ultrathin layers and the effects of Nb dopants on their TE transport properties.

Results and Discussion

The single crystals of $Mo_{1-x}Nb_xS_2$ were synthesized by the chemical vapor transport method. The shiny property and hexagonal shape (figure 1(a)) are similar to the hexagonal crystal structure of MoS_2. The smoothness and uniformity of mechanically exfoliated ultrathin layers in the atomic force microscope (AFM) image (figure 1(b)) convince the layered structure and the single crystalline of the synthesized materials.

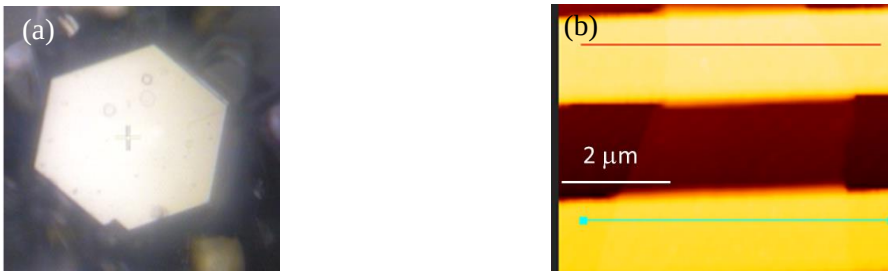

Figure 1. (a) Optical image of a $Mo_{0.97}Nb_{0.03}S_2$ flake and (b) AFM image of ultrathin layer.

The effectiveness and reliability of the fabricated devices of Nb-doped MoS_2 ultrathin layers (figure 2) are supported by ohmic contacts and the temperature profile simulated via finite-element-method software Flow 3D. Figure 3(a) shows the pseudospherical constant-temperature line profile around electrodes of the sample #1. At steady state after applying 70 mW of heater power, the temperature difference in the sample $T_2 - T_1$ is

1.37 K, meanwhile, the temperature difference of the thermometers which are the junctions of Si surface ($T_6 - T_5$ = 1.24 K) and Au electrodes ($T_4 - T_3$ = 1.27 K) is 1.255 K (figure 3(b)), where T_1, T_2, T_3, and T_4 are the temperatures at the sample above electrodes 3 and 2, and at Au electrodes 5 and 6 in sequence; T_5, T_6, T_7, and T_8 are the temperatures of Si surface beneath electrodes 5, 6, 3, and 2, respectively. The small discrepancy of 1.37 and 1.255 K probably produces an error of 8% for S measurement. Thermal resistance between the sample and electrode interface at two interfaces is negligible because this effect will be cancelled by determining the temperature difference.

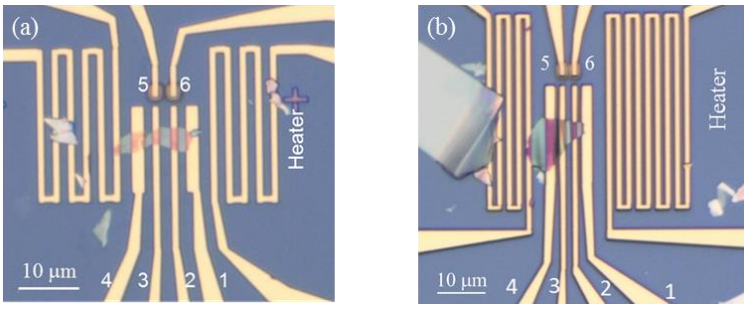

Figure 2. Optical images of (a) sample # 1 (b) sample # 2.

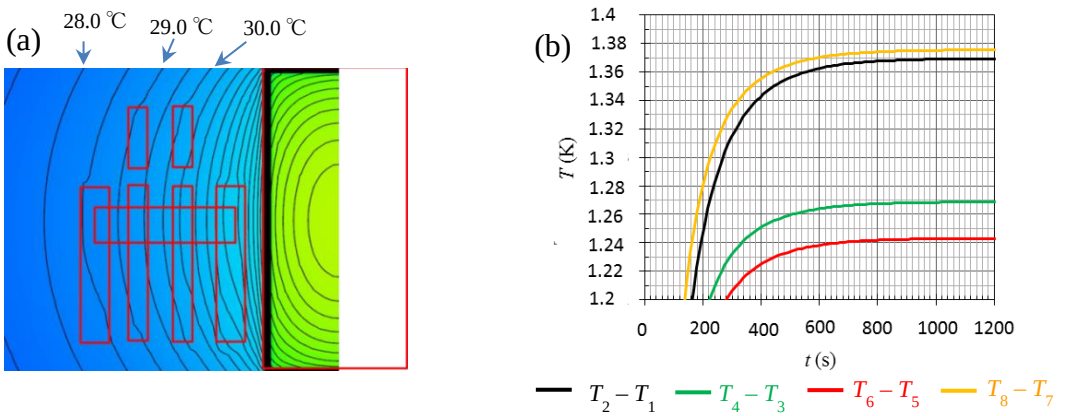

Figure 3. (a) Constant-temperature line profile surrounding the sample # 1.(d) Time-evolution of temperatures between the two significant points.

Figure 4 displays the $\rho(T)$ of two ultrathin samples: #1 and #2 with the thickness of 4.5 nm and 8 nm in sequence, and a bulk sample at 300 K. The concomitant decrease in ρ with rising T indicates the semiconducting-like behavior of the two ultrathin samples. Compared with the bulk sample at 300 K, ρ of the thin samples is about one order larger. This large increase in ρ is understood by the carrier localization effect. There localized states in a tail of the valence band above the Fermi level are caused by the random potential resulting from the Nb substitution, surface defects, and edge roughness. This assumption is consistent with Anderson's prediction [7] on weak localization (WL) theory which describes the linear dependence of electrical conductivity σ with ln$T$ as in the inset of figure 4. This result suggests that the dominant carrier conduction mechanism is WL.

Plotted in figure 5 is the temperature dependence of S of the two ultrathin layers and the bulk sample, in which S for both thin samples increases with rising T. At 300 K, S of the bulk Nb-doped MoS_2 is not so much different compared to that of ultrathin layers. Moreover, the experimentally obtained results show that the obtained S is independent of the thickness, even in a WL state. Based on the Boltzmann theory [8], the lack of change of S by layer thickness suggests that the modulation of spectral conductivity is cancelled even in the localization condition. Furthermore, the roughly linear dependence of S on T portrayed in figure 5 is consistent with the Mott relation for degenerate semiconductors [9].

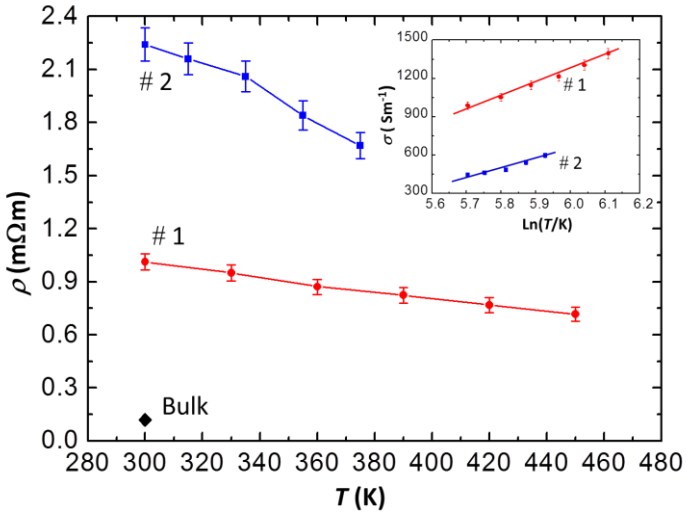

Figure 4. Temperature dependence of electrical resistivities of sample # 1, sample # 2, and bulk MoS_2. The inset displays the plot of electrical conductivity σ as a function of ln$T$.

The explanation of the physical mechanism for TE transport in the MoS_2 and Nb-doped MoS_2 ultrathin layers is supported by first-principles calculations (figure 6). The DOS of MoS_2 monolayer (black line) presents the p-type semiconducting behavior. The Fermi level is located at the top of the valence band that consists of the hybridization states of Mo 4d and S 3p orbitals. Compared to the MoS_2 monolayer, the DOS for the Nb-doped MoS_2 monolayer (red line) does not change. The small DOS peak appears at the top of the valence band due to the hybridization of Nb 4d and S 3p orbitals. The Fermi level moves to the top of this DOS peak that is consistent with the experimental picture, in which the Nb-doped MoS_2 electronic state is a p-type degenerate semiconductor.

Conclusion

This research investigates the TE properties of p-type Nb-doped MoS_2 ultrathin layers and points out the influence of Nb dopants on TE transport properties of these ultrathin layers. This research provides an effective way to fabricate the devices of Nb-doped MoS_2 ultrathin layers in which the Au with high work function, chemical stability, and good electrical conduction makes the good electrical contact with Nb-doped MoS_2 ultrathin layers. The results of this research can be applicable to elucidate the TE transport properties in doped ultratin layers and fabricate effectively the devices of p-type doped ultrathin layers for investigating TE properties.

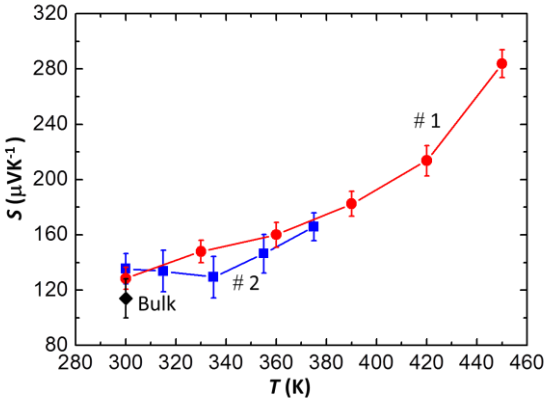

Figure 5. Temperature dependence of S of two thin samples, and bulk at 300 K.

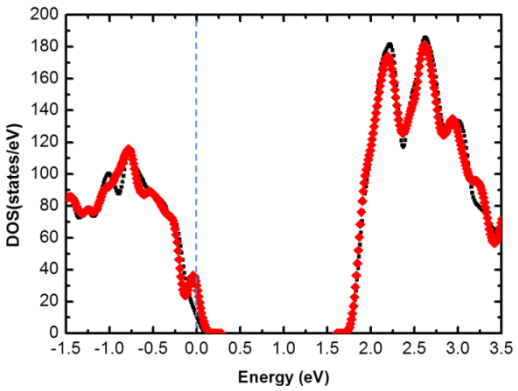

Figure 6. DOS for a 6 × 6 pristine MoS_2 supercell (black line) and a 6 × 6 MoS_2 supercell in which one Mo atom is replaced by a Nb (red line). The vertical dashed line shows the Fermi level.

Keywords: MoS_2, thermoelectric properties, ultrathin layer, weak localization, first-principles calculations.

Table of contents

References

[1] A. F. Ioffe, *Semiconductor Thermoelements, and Thermoelectric Cooling.* Infosearch, Ltd., London, 1957.

[2] A.J. Minnich *et al.*, Bulk nanostructured thermoelectric materials: current research and future prospects, *Energy & Environmental Science*, 2, 466, 2009.

[3] L. D. Hicks and M. S. Dresselhaus, Effect of quantum-well structures on the thermoelectric figure of merit, *Phys. Rev. B*, **47**, 12727 ,1993.

[4] G. R. Bhimanapati *et al.*, Recent Advances in Two-Dimensional Materials beyond Graphene, *ACS Nano*, **9**, 11509, 2015.

[5] D. Lembke *et al.*, Single-Layer MoS_2 Electronics, *Acc. Chem. Res*, **48**, 100, 2015.

[6] G. J. Snyder and E. S. Toberer, Complex thermoelectric materials, *Nat. Mater*, **7**, 105, 2008.

[7] P. W. Anderson *et al*., Possible Explanation of Nonlinear Conductivity in Thin-Film Metal Wires, *Phys. Rev. Lett.* **42**, 718, 1979.

[8] D. M. Rowe, Materials, Preparation, and Characterization in Thermoelectrics. CRC Press, Taylor & Francis Group, Boca Raton 2012, Ch. 7.

[9] O. Eibl *et al.*, Thermoelectric Bi2Te3 Nanomaterials. Wiley-VCH, Weinheim, Germany 2012, Ch. 5.

Research achievement

◆ Publication Article

Pham Xuan Thi, Masanobu Miyata, Huynh Van Ngoc, Pham Tien Lam, Nguyen Thanh Tung, Manahan Muruganathan, Phan Trong Tue, Masashi Akabori, Dam Hieu Chi, Hiroshi Mizuta, Yuzuru Takamura, and Mikio Koyano; Thermoelectric properties and carrier localization in ultrathin-layer of Nb-doped MoS_2, *Phys. Status Solidi B*, 1800125(1-8), 2018.

◆ International conference

Mikio Koyano, Wataru Asai, Pham Xuan Thi, and Masanobu Miyata, Contactless temperature measurement of atomic-layered MoS_2 single crystal supported on silicon substrate, The 37th Annual International and 16th European Conference on thermoelectrics (Cane France, 1-5 July 2018) [Poster 2, P. 74].

◆ Domestic conference

1. Pham Xuan Thi and Mikio Koyano; Growth of single crystal and mechanical exfoliation of ultrathin layer MoS_2, 2015 Thermoelectric Society of Japan (Poster presentation).

2. Pham Xuan Thi, Marek Schmidt, Phan Trong Tue, Masashi Akabori and Mikio Koyano; Fabrication of suspended ultrathin layer of $Mo_{0.97}Nb_{0.03}S_2$ for measurement of thermal conductivity, 2016 Thermoelectric Society of Japan (Oral presentation) .

◆ Other

ラマン分光法による界面熱抵抗の直接測定 浅井 渉，Pham Xuan Thi，竹内 真里美，末岡 伸一，宮田 全展，小矢野 幹夫第 65 回応用物理学会春期学術講演会（2018 年 3 月 18 日，早稲田大学西早稲田キャンパス）[9.4 応用物性・熱電変換, 18p-P3-18].